Incipient grain transport and pattern formation at a sand surface sheared by a continuous laminar flow.
Part I: Weak bed slope. Erosion dominated regimes.

T. Loiseleux[*](1,2), D. Doppler[(1)], P. Gondret[(1)] and M. Rabaud[(1)]

(1) Laboratoire Fluides, Automatique et Systèmes Thermiques (FAST) – Orsay - France
(2) Unité de Mécanique (UME) – Ecole Nationale Supérieure de Techniques Avancées (ENSTA) – Paris - France

Abstract
The destabilisation of a horizontal or tilted granular bed by a *continuous* and *laminar* hydrodynamic flow is studied experimentally in a narrow flume. The erosion threshold is investigated for various angles and grain sizes and compared to a force balance on a single grain. Above erosion threshold, the granular medium surface deforms and periodic propagating structures arise. Two regimes may be distinguished in the time evolution of these ripples. For short times, an algebraic growth is evidenced. For long times, their characteristics - amplitude, wavelength, phase velocity - exhibit a logarithmic behaviour and no saturation is observed.

1.   Introduction

The modeling of many natural phenomena - sediment transport or bedforms for instance - or industrial processes such as oil production or underwater infrastructures, demands a thorough knowledge of the coupling mechanisms between a hydrodynamic flow and a heterogeneous medium. A complete description of such interactions requires a dynamic equation for the fluid, a dynamic equation for the granular medium and a description of the boundary conditions at the interface. However, if a fluid flow description is accessible, the equations for a granular medium are an incipient physics whereas laws for granular transport as well as boundary conditions remain mostly empirical. In this context, a description of the erosion mechanism appears to be a crucial issue. Since the pioneer work of Shields (1936), many studies on the inception of erosion have been conducted. However, collected data exhibit a large dispersion partly dependent on the chosen criterion but also on the nature of the flow as underlined by White (1940). For a turbulent flow, velocity fluctuations strongly modify the instantaneous shear stress imposed to grains at a sand bed surface. Granular transport may then be observed for small mean values of the shear. For this reason, some experimental works have been devoted to erosion determination with viscous liquids in order to maintain a laminar flow such as White (1940, 1970), Mantz (1977) Yalin and Karahan (1979) or Charru *et al.* (2003). In this spirit, we carry out an experimental work on friction mechanisms at a sand bed surface sheared by a continuous water flow in a confined geometry that imposes a laminar flow. This configuration is, of course, far from natural situation, however, we expect to gain in physical understanding of the physical mechanisms by controlling the various parameters that may be implied in the erosion process.

Above erosion threshold, the sand surface deforms and patterns appear. This phenomenon has been extensively studied. However, much papers in the literature are theoretical and deal with the linear instability of a sand bed when sheared by a continuous flow: Kennedy (1963), Richard (1980), Sumer and Bakiogly (1984), Coleman and Fenton (2000), Charru and Mouilleron (2002) among others whereas very few experimental results are available: Yalin (1985), Coleman and Melville (1996), Betat *et al.* (2002), and none consider a laminar flow. In the present work, we will follow the time evolution of growing ripples induced by a continuous and laminar flow.

---

[*] Corresponding author: thomas.loiseleux@ensta.fr.

2. Experimental set-up

The experimental set-up mainly consists in a Hele-Shaw cell (Fig. 1) composed of two glass plates (length L = 130 cm and height H = 20 cm) separated by a small gap (b = 2 mm). The cell is partially filled with sifted glass beads of mean diameter d and density r_s = 2.5 10^3 kg/m^3. For a given bead size d, the dispersion in the diameter distribution remains rather narrow: $\pm$ 10 µm. These beads are fully immersed in water. As we focus on the coupling between a hydrodynamic continuous flow and the sand bed surface, there is no air in the cell in order to avoid possible interactions with free-surface waves. The hydraulic circuit is closed and composed of the Hele-Shaw cell, a filter, a centrifugal pump, a decanting tank and a calibrated flow-meter. By adjusting the pump frequency, a flow rate Q is imposed through the cell (0 = Q = 400 cm^3/s).

In order to study the effect of a bed slope on the erosion process the cell can rotate in the vertical plane. The tilt angle, denoted b, between the horizontal and the cell length direction can be modified continuously in the range [-60°, +60°] with a $\pm$ 0.1° resolution. Water flows from left to right and, by convention, b is chosen positive for water flowing uphill and negative when flowing downhill. The horizontal situation then corresponds to b = 0. The possibility to tilt the cell to large angles is used between each set of experiments to recover a flat interface by a sequence of large avalanches in both directions. All data are deduces by image processing from movies obtained by CCD cameras fixed to the cell and rotating with it.
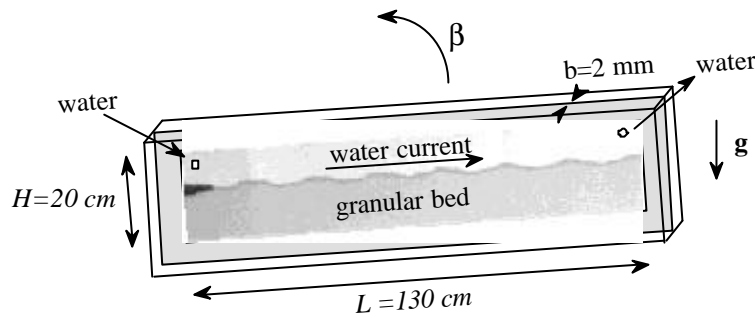

Fig. 1: Sketch of the experimental cell.

Such a confined experimental set-up is of course far from a natural situation. However, it remains a good model for studying the effect of a continuous flow on a granular bed in a well-controlled configuration. Indeed, in this narrow flume, the flow is laminar, the shear close to the granular interface is constant all along the bed and the velocity profile of the water flow is known analytically: it is parabolic across the gap b with a maximum velocity constant in the middle plan except near the upper wall or close to the interface. Gondret *et al.* (1997) showed that in such a Hele-Shaw cell the mean velocity, averaged across the gap, is equal to $\overline{U}$ in the cell but goes to zero at the lower wall exponentially with a characteristic scale equal to the cell thickness b. If we neglect the fact that the bed is rough at the grain scale and is porous (then velocity is not exactly zero at the bed surface as shown by Beavers and Joseph (1967)) the shear close to the interface is equal to $\acute{Y} \approx 3.26\overline{U}/b$ (see Gondret et al. (1997) for more precision). As the grain diameter is much smaller than the scale b of evolution of the velocity profile, we can estimate the typical velocity u_0 at the height $d/2$ over the bed where the centre of a surface bead is supposed to be located: $u_0 = \acute{Y}d/2$. These results suppose that the flow remains laminar in the cell *i.e.* that the flow Reynolds number $\text{Re}_b = r_l\overline{U}b/h$ - where h is the dynamical viscosity and r_l the liquid density - based on the mean fluid velocity $\overline{U}$ and the gap size b, remains below a minimum value of 900. This will be largely the case in the present study as Re_b < 600. However if this Reynolds number is important for determining if the bulk flow is laminar or turbulent, it is not a relevant parameter at the grain scale. A particle Reynolds number based on the grain diameter d and the typical velocity u_0 at the centre of a grain at the surface seems more appropriate:

$$\mathrm{Re}_d = \frac{r_l u_0 d}{h} = \frac{r_l \acute{g} d^2}{2h} \, .$$

Our two experimental control parameters are the flow rate Q and the tilt angle $\textbf{\textit{b}}$. From Q and the height of flowing water (~ 10 cm) we deduce the mean water velocity $\overline{U}$, the shear $\acute{g}$ and the velocity u_0. For water flowing typically at $\overline{U} = 20 \, cm/s$, $\mathrm{Re}_b = 400$ and $\mathrm{Re}_d = 36$ for 180 µm beads. These two values show that the hydrodynamic flow above the interface remains laminar and that the wake of an individual motionless grain is transitional (the wake is close to become time dependant) with a typical inertial drag coefficient C_D of the order of 5.

In the literature concerned with erosion process the classical dimensionless number to describe the onset is the Shields number (Shields, 1936). This parameter is the ratio between tangential and normal stresses acting on a grain. For a laminar flow, the viscous tangential stress is proportional to the velocity gradient, the normal stress being, as usual, the apparent weight of a grain. Shields number then writes:

$$\textbf{\textit{q}} = \frac{h\acute{g}}{\Delta r g d} \, ,$$

with $\Delta r = r_s - r_l$ (indices s and l stand for solid and liquid).

3   Erosion thresholds

3.1   Description and experimental results

At low flow rates, grains are motionless. For large flow rates, layers of beads are dragged by the flow and the sand bed surface is strongly eroded and deformed. For a specific flow rate Q, some beads are intermittently extracted from the bed surface. The number of moving grains is erratic. At a given instant, no grain may move at the interface. However, transport will rapidly start again. This is our definition of erosion threshold. Note that a transient erosion state below Q_c exists as evidenced by Mouilleron (2002): some grains move but the process rapidly stops definitively.

The critical Shields for erosion θ_c is presented Fig. 2, for different grain sizes, as a function of the bed slope β. All curves $\theta_c(\beta)$ exhibit the same trend for different grain diameters in the range 110 µm = d = 220 µm. The effect of tilting the cell is, in accordance with intuition, to increase the onset of erosion for positive slope and to decrease it for negative slope. Although this effect is almost linear with the tilt angle between –20°<$\textbf{\textit{b}}$<+20° it presents a maximum for $\textbf{\textit{b}}$ ~ +20°, as if, when $\textbf{\textit{b}}$ becomes close to the angle of avalanche (~ ± 30°), surface grains were easier to force out. The same destabilising effect is also observed for $\textbf{\textit{b}}$ < - 20° when gravity act in the flow direction. In both cases this weakening effect appears clearly before the slope reaches the natural angle of avalanche.
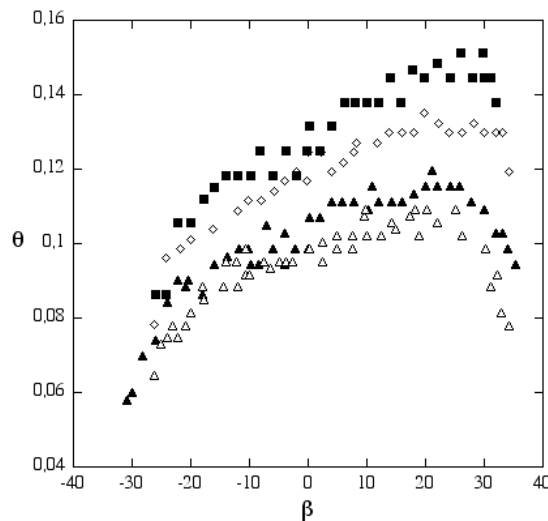

Fig. 2: Critical Shields number for erosion as a function of the cell angle for various grain diameters:
(■) d = 110 µm, (◊) d = 140 µm, (▲) d = 180 µm, (?) d=220 µm.

3.2 Erosion model

If we consider a single bead on a plane inclined by an angle b, submitted to an uphill flow, three forces govern its equilibrium (Fig. 3):

(i)   Its apparent weight, $\mathbf{F}_W = \dfrac{pd^3}{6}\Delta rg$.

(ii)   The drag force $\mathbf{F}_D$. Since the particle Reynolds number Re_d is relatively small we can write $F_D = a\,3ph\,du_0 f(\mathrm{Re}_d)$ where $3\pi h d u_0$ stands for the Stokes force on a sphere in a homogeneous and infinite flow of velocity u_o. The term $f(\mathrm{Re}_d)$ is a corrective factor to the Stokes drag when the Reynolds number is not very small. It tends towards 1 for vanishing Re_d and towards $C_D\mathrm{Re}_d/24$, with a corresponding drag coefficient $C_D \sim 0{,}4$, when Re_d goes to infinity. In the Reynolds range $[0, 1000]$, a good fit for $f(\mathrm{Re}_d)$ is the empirical law $f(\mathrm{Re}_d) = 1 + 0.15\,\mathrm{Re}_d^{0.687}$ (Clift *et al.*, 1978). The constant α takes into account the particular geometry and more precisely the fact that the grain is close to a surface and moreover a rough one. For a smooth or rough sphere on a plane submitted to a constant gradient velocity field, O'Neill (1968) and more recently King and Leighton (1997) obtained the value $a \sim 1.70$. However, this coefficient is certainly smaller in the present case as the sphere is on other grains and is consequently partially shielded from the shear stress.

(iii)   The friction force F_f: Its maximum value can be modelled by a Coulomb force in opposite direction to the flow, proportional to the normal force, $\mathbf{F}_f = m(\mathbf{F}_W)_\perp$, where $m = \tan d$ is the friction coefficient and δ the friction angle.
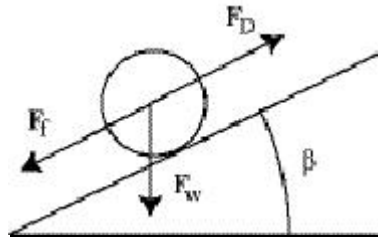

Fig. 3: Sketch of forces acting on a motionless grain located in an uphill flow on a smooth bed tilted by an angle β.

For a motionless grain but just about to move, the balance of forces along the bed in the direction of the flow writes:

$$-\frac{pd^3}{6}\Delta rg\sin b - m\frac{pd^3}{6}\Delta rg\cos b + a\,3ph\,du_0 f(\mathrm{Re}_d) = 0$$

which leads to the critical Shields number for the incipient motion of a grain:

$$q_c = \frac{1}{9af(\mathrm{Re}_d)}\frac{\sin(b+d)}{\cos(d)}. \qquad (1)$$

This onset value is then a function of the bed slope β, of the friction angle δ and of the particle Reynolds number Re_d. We can now compare this value to the experimental onset of erosion obtained for horizontal or tilted cells. Note that this model is valid for positive or negative b as the friction force F_f remains in both cases opposite to the drag force F_D.

3.2.1 Horizontal bed

When the bed is horizontal ($b = 0$), equation (1) reduces to:

$$q_0 = \frac{\tan(d)}{9af(\mathrm{Re}_d)}. \qquad (2)$$

This function is presented Fig. 4 as a function of Re_d with the two asymptotes corresponding to small and large particle Reynolds numbers. Our experimental results for a horizontal interface are also plotted, as

well as a recent result by Charru *et al.* (2003) obtained on a circular configuration with a laminar flow.
The agreement between the model and the data is very satisfactory for $a = 0.44$. Smaller than the value determined by O'Neill (1968), this result seems nevertheless very sensible. Indeed, as already mentioned, the bead is not lying on a smooth plane but partially buried in the surface of the bed. Note that these values of the critical Shields corresponding to laminar flow are significantly larger that those corresponding to turbulent flows (see for example Fig. 5 of Yalin and Karahan (1979)).

3.2.2   Tilted bed

Our simple model gives also the evolution of the critical Shields number q_c as a function of the bed slope (Eq. 1). If we normalise q_c by q_0, the Shields corresponding to a horizontal interface, this writes:

$$\frac{q_c}{q_0} = \frac{f(\mathrm{Re}_{d0})}{f(\mathrm{Re}_d)}\frac{\sin(b+d)}{\sin(d)} \qquad (3)$$

where Re_{d0} is the particle Reynolds number at onset for $b = 0$. Now if we assume that the variation of the viscous drag coefficient between Re_{d0} and Re_d is negligible, which is suggested by the form of f, Eq. (3) becomes:

$$\frac{q_c}{q_0} \approx \frac{\sin(b+d)}{\sin(d)} \qquad (4)$$

Note that this equation has already been obtained in previous studies. Indeed the effect of a bedslope on the bed-load transport has been investigated and modelled by different authors such as Allen (1982) or Dyer (1986) for instance. There analysis based on the forces or on the moments of forces acting on a single grain laying on two beads in a turbulent flow lead to equations of the same form than Eq. (4).

We can now compare on Fig. 5 the prediction of Eq. (4) with the experimental data of Fig. 2 re-normalised by the values of q_0. The experimental data collapse on a master curve and are in good accordance with Eq. (4) except that the strong decrease of the critical Shields number for $|b| > 25°$ is not predicted. Besides, a fit by Eq. (4) gives $d ˜ 69°$. This value is surprisingly high since a typical value of the order of the natural angle of avalanche (˜ 30°) would have been anticipated. All appears as if the friction coefficient in the presence of a flow, uphill or downhill, was strongly increased. This result is confirmed by previous experimental results of Whitehouse and Hardisty (1988) giving also a similar large value of d.
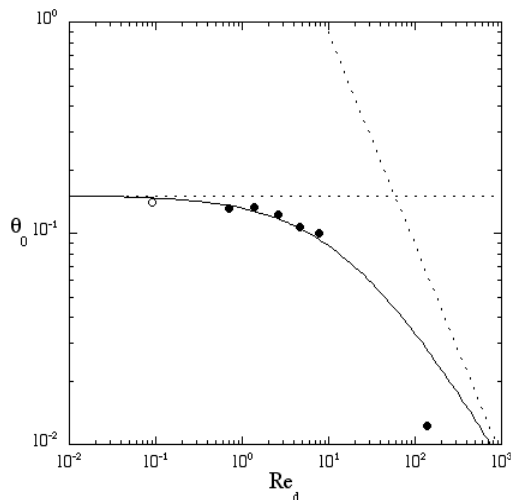

Fig. 4: Critical Shields number $?_0$ for erosion on a horizontal bed as a function of Re_d. Continuous line corresponds to Eq. (1) for $?? = 0.44$ and dotted lines to the asymptotic behaviours at small and large Re_d. Comparison with our experimental data: (v) and result by Charru *et al.* (2003): (O).
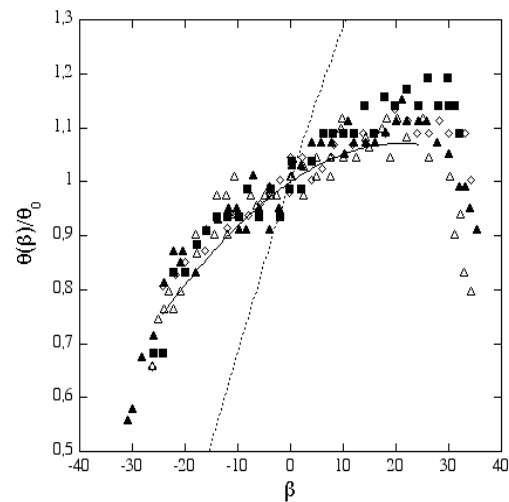
Fig. 5: Evolution of the experimental ratio $???_0$ of the erosion onset as a function of the slope $?$ for various grain diameters (same data as in Fig. 2) and curves given by Eq. (4) in the range [- 25°, 25°] obtained for friction angle $? = 30°$ (------) and $? = 69°$ (———), corresponding respectively to the expected value of $?$ and to the best fit

for all data.

4 Pattern characteristics

Above erosion threshold, the interface does not remain flat. Periodic ripples of triangular shape arise and grow as evidenced on Fig. 6. When formed, grains roll along the upstream slope of the ripples and fall in avalanche on their downstream slopes.
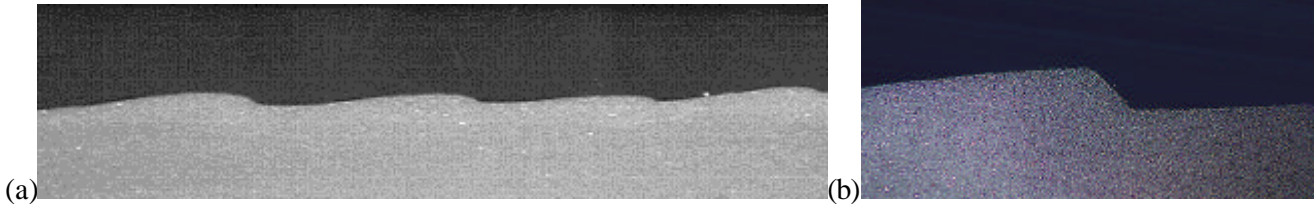
(a)   (b)

Fig. 6 - (a) Visualisation of periodic triangular ripples propagating from left to right. (b) Zoom on a single ripple. d = 110 µm, θ = 0.15, β =0°.

The position of the entire sand/fluid interface is followed in time and space, and the ripple characteristics are deduced by image processing. The mean time evolution of the ripple amplitude A, wavelength λ and velocity displacement c is presented Fig 7 for a unique grain size d=110 µm and for four flow intensities above erosion threshold on a horizontal bed configuration (β=0). Data are averaged values for several runs and over all ripples for each run. Note that, even in this configuration, the determination of ripple heights and velocities remains difficult at the early stages. The mean wavelength is the most precise characteristics. These structures propagate in the stream direction; they grow in amplitude and in wavelength during their motion all along the cell while they propagate more en more slowly. The dynamics is more rapid when the distance to thresholds $\Delta = (q - q_0)/q$ is increased.
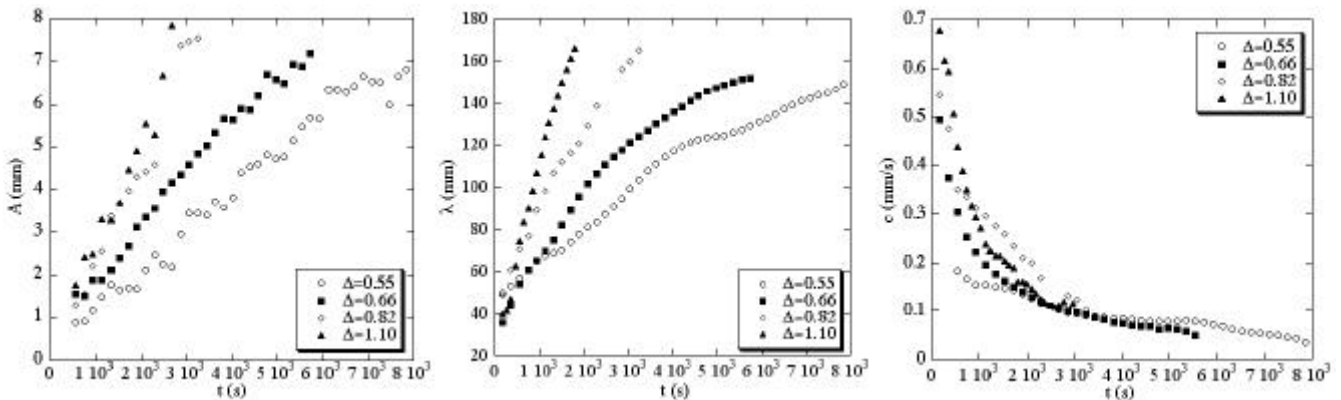
Fig. 7: Time evolution of ripple characteristics – amplitude A, wavelength λ and velocity displacement c – for four non-dimensional flow rates $\Delta = (q - q_0)/q$. d=110 µm.

Two regimes may be distinguished in the time evolution of these erosion patterns as shown Fig. 8. For short times, ripple characteristics evolve linearly with time. This slow initial growth is not in accordance with much theoretical approaches that model the destabilisation of the sand/fluid interface with a linear stability approach, corresponding to an initial exponential growth of the structures. As evidenced Fig. 8, the long time behaviour of the ripples is logarithmic. No saturated state may be reached in this configuration. Hence, for given flow rate, grain size and tilt angle, structures cannot be characterised by a unique height, length and displacement velocity.

Note that, for all distance to thresholds Δ studied, the change of regime always occurs when the ripples reach the amplitude A=1.8 +/- 0.3 millimetres. It also corresponds to a change in the shape of the ripples and more precisely to the appearance of a real slip face at the downstream front of the ripples. Most

probably, this modification in the time evolution is closely connected to the growth of a flow separation behind each ripple. A such effect has already been evidenced by Rousseaux (2003) between rolling grain ripples and vortex ripples regimes in an oscillating configuration.
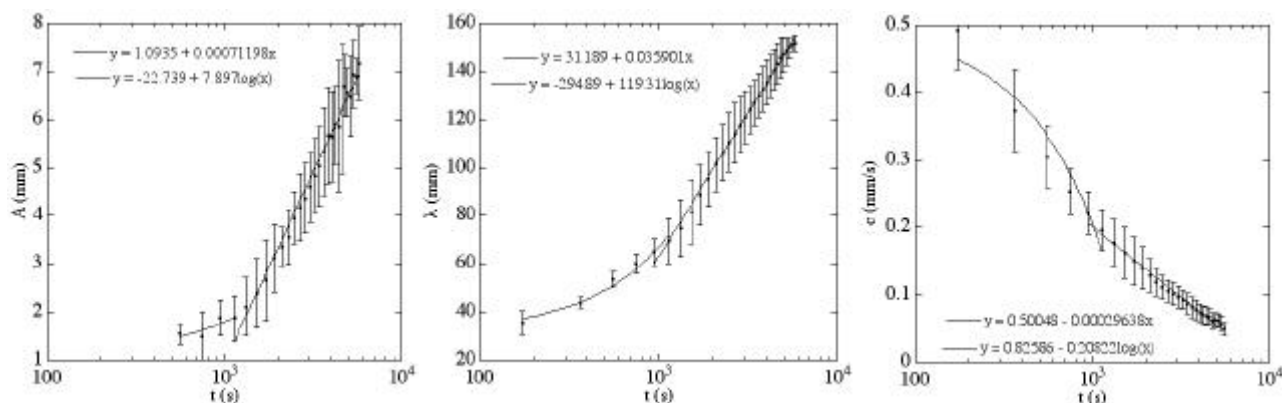

Fig. 8: Time evolution of ripple characteristics in a log-lin scale. d=110 mm, Δ=0.66.

5.   Discussion and conclusion

In this article, we studied the effect of a continuous laminar hydrodynamic flow on a granular bed in a very confined geometry and well-controlled configuration. The erosion thresholds for various grain sizes determined experimentally for a horizontal bed ($\beta = 0$) are in very good agreement with a model based on a force balance on a single grain. When a non-zero slope ($\beta \neq 0$) is imposed, the same model fail to reproduce the experimental data for a coherent friction angle δ. For the moment, we cannot find any plausible physical interpretation for explaining the too large value of d given by the model. Including a lift force in the force balance, as suggested by King and Leighton (1997), does not significantly modify the results. A negative lift due to the flow above the bead could increase the normal stress and consequently the apparent friction coefficient. However the necessary value for this negative lift seems totally unrealistic. A less crude model is probably necessary for a correct matching with experimental data.

Above erosion thresholds, ripples that arise have been followed in time for different shear stresses. The observed behaviour – algebraic for short times, logarithmic for long times – is somewhat peculiar and cannot be compared to any known model of ripple growth or evolution. A new approach needs to be developed based on other concepts than linear stability.

Acknowledgements

References

J. R. L. Allen, Simple models for the shape and symmetry of tidal sand waves 1, 2 et 3, *Marine geology* 48, 31-49, 1982.

A. Betat, V. Frette and I. Rehberg, Long-time behaviour of sand ripples induced by water shear flow, *Eur. Phys. J. E* 8:465-476, 2002.

G. S. Beavers and D. D. Joseph, Boundary conditions at a naturally permeable wall, *J. Fluid Mech* 30, 197-207, 1967.

F. Charru and H. Mouilleron-Arnould, Instability of a bed of particles sheared by a viscous flow, *J. Fluid Mech.* 452, 303-323 2002.

F. Charru, H. Mouilleron-Arnould and O. Eiff, Erosion and deposition of particles on a bed sheared by a viscous flow, *J. Fluid Mech*, Submitted, july 2003.

R. Clift, J. R. Grace and M. E. Weber, Bubbles, drops and particles, *Academic Press*, 1978.

S. E. Coleman and J. D. Fenton, Potential-flow instability theory and alluvial stream bed forms, *J. Fluid Mech.* 418:101-117, 2000.

S. E. Coleman and B. W. Melville, Initiation of bed forms on a flat sand bed, *J. Hydr. Engng ASCE* 122:301-310, 1996.

K. R. Dyer, Costal and estuarine sediment dynamics, *Wiley*, 1986.

P. Gondret, N. Rakotomalala, M. Rabaud, D. Salin and P. Watzky, Viscous parallel flows in finite aspect ratio Hele-Shaw cell: analytical and numerical results, *Phys. Fluids* 9,1841-1843, 1997.

J. F. Kennedy, The mechanics of dunes and antidunes in erodible-bed channel, *J. Fluid Mech.* 16:521-544, 1963.

M.R. King and D.T. Leighton, Measurement of the inertial lift on a moving sphere in contact with a plane wall in a shear flow, *Phys. Fluids* 9, 1248-1255, 1997.

P.A. Mantz, Incipient transport of fine grains and flakes by fluids – Extended Shields diagram, *Journal of the Hydraulics Division, ASCE*, 103, 601-615, 1977.

M.E. O'Neill, A sphere in contact with a plane wall in a slow linear shear flow. *Chem. Eng. Sci..* 23: 1293–1298, 1968.

K.L. Richards, The formation of ripples and dunes on an erodible bed, *J. Fluid Mech.* 99, 597-618, 1980.

G. Rousseaux, Etude de l'instabilité d'une interface fluide-granulaire : Application à la morphologie des rides de plages, PhD thesis, Université Paris 6, 2003.

A. Shields, Anwendung der Ahnlichkeitsmechanik und der Turbulenzforschung auf die Geschiebebewegung, *Heft 26. Preuss. Vers. für Wasserbau und Schiffbau, Berlin,* 1936.

C. M. White, The equilibrium of grains on the bed of a stream, *Proc. Roy. Soc. Lond.* 174A:322-338, 1940.

C. M. White, Plane bed thresholds of fine grained sediments, *Nature* 228:152, 1970.

Whitehouse R.J.S. and Hardisty J., Experimental assessment of two theories for the effect of bedslope on the threshold of bedload transport. *Marine Geology* 79, 135-139, 1988.

M. S. Yalin and E. Karahan, Inception of sediment transport. *J. Hydraul. Div., Am. Soc. Civil Eng.* 105: 1433–1443, 1979.

M. S. Yalin, On the determination of ripple geometry, *J. Hydr. Engng ASCE* 111:1148-1155, 1985.